Supplementary Materials for

Clonal hematopoiesis associated with Tet2 deficiency accelerates atherosclerosis development in mice

José J. Fuster*, Susan MacLauchlan, María A. Zuriaga, Maya N. Polackal, Allison C. Ostriker, Raja Chakraborty, Chia-Ling Wu, Soichi Sano, Sujatha Muralidharan, Cristina Rius, Jacqueline Vuong, Sophia Jacob, Varsha Muralidhar, Avril A. B. Robertson, Matthew A. Cooper, Vicente Andrés, Karen K. Hirschi, Kathleen A. Martin and Kenneth Walsh*

* Correspondence to: jjfuster@bu.edu or kxwalsh@bu.edu

This PDF file includes:

Materials and Methods

Mice

C57Bl/6J Ldlr-deficient mice (Ldlr-/-), C57Bl/6J Tet2-deficient mice (Tet2-/- and +/-) (13), C57Bl/6J LysM-Cre mice, C57Bl/6J Tet2 floxed mice (14) and C57Bl/6 Cd45.1 Pep Boy mice were obtained from Jackson Laboratories. Female mice were used for *in* vivo experiments unless otherwise noted. Mice were maintained on a 12-h light/dark schedule in a specific pathogen-free animal facility and given food and water *ad libitum*. The number of mice included in each study is indicated in the figures or the associated legends. The Institutional Animal Care and Use Committee of Boston University approved all study procedures.

Competitive bone marrow transplantation and atherosclerosis induction

Lethally irradiated Ldlr-/- recipients were transplanted with suspensions of BM cells containing 10% CD45.2+ Tet2-/- cells and 90% CD45.1+ Tet2+/+ cells (10% KO-BMT mice), or 10 % CD45.2+ Tet2+/+ cells and 90% CD45.1+ Tet2+/+ cells (10% WT-BMT mice) (Fig.S1). BM cells were isolated from femurs and tibias of donor mice after euthanasia. Donor CD45.2+ cells were obtained from Tet2+/+ or -/- littermates; donor CD45.1+ cells were obtained from Pep Boy mice. Recipient Ldlr-/- mice were irradiated in a pie cage (Braintree Scientific) to limit mobility and ensure equal dose of irradiation, and were exposed to two radiation doses of 550 rad three hours apart using an X-RAD 320 Biological Irradiator. After the second irradiation, each recipient mouse was injected with 10^7 BM cells i.v. Sterilized caging, food and water were provided during the first 14 days post-transplant and water was supplemented with antibiotics (Sulfatrim). Mice that did not recover full pre-irradiation body weight 28 days after transplant were excluded from further analysis. Starting four weeks after BMT, mice were fed a high fat high cholesterol (HFHC) Western diet (Harlan-Teklad, TD.88137, Adjusted Calories Diet; 42% from fat, 0.2% cholesterol) to promote hypercholesterolemia and the development of atherosclerosis. Mice were maintained on a HFHC diet for 9 weeks, unless otherwise noted. As control, a subset of mice was fed a normal rodent diet for the same period of time (Harlan-Teklad, 2014 rodent maintenance diet). In addition, in a subset of experiments this same competitive BMT strategy was used to evaluate the effects on atherosclerosis of the clonal expansion of Tet2+/- cells (10% HET-BMT).

Generation of myeloid-restricted Tet2-deficient mice

Mice with myeloid-restricted Tet2 ablation were generated by crossing Tet2-floxed mice ($Tet2^{flox/flox}$) with LysM-Cre mice. BM samples from $LysMCre^{+}$ $Tet2^{flox/flox}$ and $LysMCre^{-}$ $Tet2^{flox/flox}$ were transplanted into Ldlr-/- recipients as described above to generate atherosclerosis-prone Mye-Tet-KO mice and WT controls, respectively.

Assessment of systemic metabolism

Plasma was collected in EDTA-coated tubes and cholesterol levels were determined using an enzymatic assay (Cholesterol E, WAKO Diagnostics). Blood glucose levels were measured with an Accu-Chek glucometer (Roche Diagnostics). Insulin tolerance tests (ITT) were performed on 5 h-fasted mice injected intraperitoneally with 0.6U/Kg human insulin (Humulin R, Eli Lilly), and blood glucose levels were measured immediately before and 15, 30, 60, 90, and 120 minutes after glucose injection

Quantification of atherosclerosis burden

Mice were euthanized and aortas were removed after in situ perfusion with phosphate-buffered saline (PBS) injected through the left ventricle of the heart. Tissue fixation was achieved by immersion in 4% paraformaldehyde in PBS overnight at 4°C. Aortic tissue was then dehydrated and embedded in paraffin for sectioning. All histological sections comprising the aortic root as determined by the location of the aortic valve leaflets were cut at a thickness of 6 μm. An operator who was blinded to genotype quantified plaque size in aortic root sections by computer-assisted morphometric analysis of microscopy images acquired on a Keyence BZ-9000 microscope. For each mouse, atherosclerosis plaque size in aortic root cross-sections was calculated as the average of 5 independent sections separated by ~18 μm. Samples which exhibited evidence of artefactual tissue damage or abnormal orientation that could not be compensated by the analysis of multiple independent sections were excluded from analysis.

Immunohistochemical analysis of atherosclerotic plaque composition.

Plaque composition was examined by immunohistochemical techniques performed by a researcher blinded to genotype. Vascular smooth muscle cells (VSMCs) were identified with mouse anti-smooth muscle α-actin (SMA) monoclonal alkaline phosphatase-conjugated antibody (clone 1A4, SIGMA) and Vector Red Alkaline Phosphatase Substrate (Vector Laboratories). Macrophages were detected with a rat anti-Mac3 monoclonal antibody (clone M3/84, Santa Cruz Biotechnologies), followed by biotin-conjugated goat anti-rat secondary antibody (Santa Cruz Biotechnologies), streptavidin-HRP (Vector Laboratories) and DAB substrate (Vector Laboratories). Specimens were counterstained with hematoxylin. Collagen content was determined by a modified Masson's trichrome staining with Fast Green as collagen stain. Microscopy images were acquired on a Keyence BZ-9000 microscope and analyzed using ImageJ software using the Color Deconvolution plugin.

Assessment of plaque cell proliferation, apoptosis and necrosis

Cell proliferation within atherosclerotic plaques was assessed by double immunofluorescent staining with monoclonal antibodies against the proliferating cell antigen Ki-67 (clone SP6, Vector Laboratories) and the macrophage marker CD68 (Clone FA-11, AbD Serotec). After deparaffinization, antigen retrieval and blockade of non-specific interactions (5% horse serum in PBS, 45 min), histological sections were incubated for 2 h at 37 °C with primary antibodies. CD68 was visualized with Alexa Fluor 488-conjugated anti-rat IgG and Ki-67 with Alexa Fluor 635-conjugated anti-rabbit IgG (both from Life Technologies). Nuclei were stained with DAPI and slides were mounted in SlowFade Gold Antifade Reagent (Life Technologies) to acquire images on a Leica SP5 confocal microscope fitted with a 40× oil-immersion objective. Settings were adjusted to maximize the signal-to-noise ratio. The sequential mode was used for image acquisition in order to avoid any interference from overlapping fluorescence. Images were analyzed with ImageJ software by a researcher who was blinded to genotype. Plaque apoptosis was determined using the terminal deoxynucleotidyl transferase dUTP nick-end labelling (TUNEL) method, following the manufacturer's recommendations (In Situ Cell Death Detection Kit Fluorescein, Roche). Images were acquired on a Keyence BZ-9000 microscope. Necrotic core extension in the plaque was evaluated by quantifying acellular collagen-free area in Masson Trichrome-stained sections.

Flow cytometry analyses of blood and tissue samples.

Peripheral blood was obtained from the facial vein. Bone marrow cells were flushed out of two femurs and two tibias per mouse. Spleen and mediastinal lymph nodes were gently pressed through a 70 μm cell strainer in PBS containing 5% fetal bovine serum (FBS) to prepare single cell suspensions. Aortic arches were digested for 45 minutes at 37°C in RPMI containing 10% FBS and 0.25 mg/ml Liberase TM (Roche Life Science). The following fluorescent antibodies were used for staining and flow cytometry analysis: eFluor450-conjugated anti-CD45.2, FITC-conjugated anti-CD45.2, Pe-Cy7-conjugated anti-CD45.1, FITC-conjugated anti-CD11b, eFluor450-conjugated anti-CD11B, PE-conjugated anti-CD115, APC-conjugated anti-CD3, FITC-conjugated anti-Lineage cocktail, APC-conjugated anti-CD69, APC-conjugated anti- Foxp3, FITC-conjugated anti-CD4, PE-conjugated anti-CD25 (from eBioscience); APC-Cy7-conjugated anti-B220, PerCP-Cy5.5-conjugated anti-Ly6G, PE-Cy7-conjugated anti-c-Kit, AlexaFluor647-conjugated anti-Sca-1, BUV737-conjugated anti-CD62L (from BD Biosciences); APC-conjugated anti-F4/80 (from R&D Systems); PerCP-Cy5.5-conjugated anti-CD45.1, BV421-conjugated anti-CD44, BV510-conjugated anti-CD8a, BV421-conjugated anti-CD127 (from BioLegend). HPSCs were identified as Lineage-, c-Kit+, Sca1+; monocytes, monocytes, as CD45+, CD11b+, CD115Hi; neutrophils, as CD45+, CD11b+, $CD115^{Lo}$, Ly6g+, T lymphocytes as CD45+, CD11B-, B220-, CD3+; B lymphocytes as CD45+, CD11b-, CD3-, B220+; aortic macrophages as CD45+, CD11B+, $F4/80^{Hi}$, effector memory T cells as $CD44^{Hi}$ CD62-, naïve T cells as $CD44^{Lo}$ CD62L+, and regulatory T cells as CD4+ $CD127^{Lo}$ CD25+ FoxP3+. Fixation/permeabilization for Foxp3 detection was achieved using commercially available kits following manufacturer's instructions (Foxp3/Transcription Factor Fixation/Permeabilization Concentrate and Diluent, eBioscience). Dead cells were excluded from analysis by DAPI staining in unfixed samples and by LIVE/DEAD Fixable Near-IR staining (ThermoFisher Scientific) in fixed samples. 123count eBeads (eBioscience) were used to quantify absolute cell numbers. A BD LSR II Flow Cytometer (BD Bioscience) was used for data acquisition. Data were analyzed with FlowJo Software.

Cell culture studies

Thioglycollate-elicited macrophages were obtained from the peritoneal cavity of mice 4 days after intraperitoneal injection of 1 ml aged 4% Brewer's thioglycollate broth (BD Difco). Macrophages were allowed to adhere for 6 hours and cultured in RPMI medium supplemented with antibiotics and 10% FBS (Perfomance Plus FBS, Gibco). Bone marrow-derived macrophages were obtained from suspensions of femoral BM that were differentiated for 7 days in the presence of RPMI medium supplemented with antibiotics, 10% FBS and 15% L929-cell conditioned medium as a source of macrophage colony-stimulating factor (MCSF). Cell cycle progression and apoptosis of cultured macrophages was evaluated by flow cytometry analysis of DNA content. After fixation in 80% ethanol for 1 h at -20ºC, cells were incubated for 30 min with 50 μg/mL propidium iodide containing 0.25 mg/mL RNAse A (both from SIGMA). For cell cycle analysis, DNA histograms were fitted into cell cycle distributions using the ModFit 3.0 software (Verity Software House). For analysis of apoptosis induced by treatment with 7-ketocholesterol (Sigma), hypodiploid (SubG1) cells were quantified using with FlowJo Software. Uptake of fluorescent DiI-conjugated oxLDL (Alfa Aesar) was evaluated by flow cytometry

analysis. Pro-inflammatory activation of macrophages was achieved by treatment with various combinations and doses of multiple stimuli as described in main text and figure legends. The following stimuli were used: LPS (Invivogen), recombinant IFNγ protein (Peprotech), oxLDL (Alfa Aesar) and recombinant TNF protein (Peprotech). For NLRP3 inflammasome activation, LPS/IFNγ-primed macrophages were treated with 5mM ATP (SIGMA) for 15 or 30 minutes. Alternatively, macrophages were treated for 8 hours with a combination of oxLDL, TNF, IFNγ and cholesterol crystals. For cholesterol crystal preparation, cholesterol (Sigma) was dissolved in 95% Ethanol, heated to 60° and cooled down at room temperature to allow crystallization; crystals were collected by filtering. Transient overexpression of GFP, wild-type Tet2 and catalytically-inactive mutant Tet2 (H1302Y, D1304A) in thioglycollate-elicited peritoneal macrophages was achieved by plasmid transfection using a Nucleofector 2b device and a Mouse Macrophage Nucleofector Kit (both from Lonza). 2.5 μg of plasmid DNA were used to transfect 10^6 macrophages. pcDNA3-Tet2 was a gift from Yi Zhang (Addgene plasmid # 60939) and catalytically-inactive mutant Tet2 was generated by site-directed mutagenesis (Q5 Site-Directed Mutagenesis Kit).

Gene expression analysis by qRT-PCR.

Total RNA from tissues and cultured cells was isolated using QIAzol reagent and RNeasy kits (QIAGEN). RNA (0.3-1.5 μg) was reverse transcribed with iScript™ Advanced cDNA Synthesis Kit kits (Bio-Rad). qRT-PCR was performed with Power SYBR® Green reagent (ThermoFisher Scientific) in a ViiA7 PCR system. Primers for mouse gene expression studies are shown below. Results were analyzed with the ΔΔCt method. 36B4, β-actin, TBP or the combination of 36B4 and β-actin were used as reference genes for normalization. The following primers were used:

Gene	Forward Primer	Reverse Primer
36B4	GCTCCAAGCAGATGCAGCA	CCGGATGTGAGGCAGCAG
β-actin	GGCTGTATTCCCCTCCATCG	CCAGTTGGTAACAATGCCATGT
TBP	CTTCCTGCGACAATGTCACAG	TCTTTCTCATGCTTGCTTCTCTG
IL-1β	TGACAGTGATGAGAATGACCTGTTC	TTGGAAGCAGCCCTTCATCT
IL-6	GCTACCAAACTGGATATAATCAGGA	CCAGGTAGCTATGGTACTCCAGAA
IL-1α	GCACCTTACACCTACCAGAGT	AAACTTCTGCCTGACGAGCTT
IL-18	CAAACCTTCCAAATCACTTCCT	TCCTTGAAGTTGACGCAAGA
TNF	CGGAGTCCGGGCAGG	GCTGGGTAGAGAATGGATGAA
CCL2/MCP1	CAGCCAGATGCAGTTAACGC	GCCTACTCATTGGGATCATCTTG
CXCL1	CCGAAGTCATAGCCACACTCAA	CAAGGGAGCTTCAGGGTCAA
CXCL2	TGACTTCAAGAACATCCAGAGCTT	CTTGAGAGTGGCTATGACTTCTGTCT
CXCL3	TTTGAGACCATCCAGAGCTTGA	CCTTGAGAGTGGCTATGACTTCTGT
CCL3	GCGCCATATGGAGCTGACA	CGTGGAATCTTCCGGCTGTA
CCL5	CAGCAGCAAGTGCTCCAATC	CACACACTTGGCGGTTCCTT
COX2	TGGTGCCTGGTCTGATGA	GTGGTAACCGCTCAGGTGTTG
SR-A	TCAGACTGAAGGACTGGGAACA	GGAGGCCCTTGAATGAAGGT
CD36	TGCCCATGCCGAGAGTCT	CAGAGGCGCACCAAACCT
ABCA1	CGTTTCCGGGAAGTGTCCTA	GCTAGAGATGACAAGGAGGATGGA

ABCG1	TCACCCAGTTCTGCATCCTCT	GCAGATGTGTCAGGACCGAGT
SELP	CATCTGGTTCAGTGCTTTGATCT	ACCCGTGAGTTATTCCATGAGT
SELE	ATGCCTCGCGCTTTCTCTC	GTAGTCCCGCTGACAGTATGC
ICAM1	GTGATGCTCAGGTATCCATCCA	CACAGTTCTCAAAGCACAGCG
VCAM	TAGAGTGCAAGGAGTTCGGG	CCGGCATATACGAGTGTGAA
NLRP3	ATTACCCGCCCGAGAAAGG	TCGCAGCAAAGATCCACACAG
PYCARD	GACAGTGCAACTGCGAGAAG	CGACTCCAGATAGTAGCTGACAA
CASP1	ACAAGGCACGGGACCTATG	TCCCAGTCAGTCCTGGAAATG

Gene expression analysis by microarrays

Total RNA from Tet2-/- and +/+ macrophages was isolated using an AllPrep DNA/RNA Mini Kit (Qiagen), and checked for quality prior to submission to the Boston University Medical Campus Microarray Core Facility. The samples were amplified, labeled and hybridized on 6 Mouse Gene 2.0 ST arrays (Affymetrix, Santa Clara, CA) per the manufacturer's instructions. Gene level signal values were normalized together using the Robust Multiarray Average (RMA) algorithm, and annotated to BrainArray Cdf files (28) using affyPLM package (version 1.34.0) included in the Bioconductor software suite (v. 2.12). Differential expression was assessed using the moderated pairwise t test implemented in the limma package (version 3.14.4). Both .cel files and expression values were deposited into MIAME compliant NCBI Gene Expression Ominus with accession number: GSE81398. Multiple hypothesis testing was performed by calculating the Benjamini-Hochberg false discovery rate and an additional filtered FDR q-value was calculated after removing genes that were expressed below array-wise median value to reduce the probability of producing false positive results. In this study, genes with a fold change $\geq$1.5 or $\leq$-1.5 fold with a filtered q-value<0.05 were considered as statistically significant differentially expressed genes (DEG). The list of DEG was uploaded to Panther Classification System for statistical overrepresentation test using default settings (29). Heap map was generated by using GENE-E software from Broad Institute (http://www.broadinstitute.org/cancer/software/GENE-E/index.html).

Analysis of cytokine secretion

IL-6 and IL-1β were analyzed in macrophage culture supernatants using commercial enzyme-linked immunoabsorbent assays (ELISA) according to manufacturer's instructions (R&D Systems).

Fluorescent staining of IL-1β and active caspase 1 in atherosclerotic plaques

Unfixed aortic tissue from HFHC-fed mice was embedded in optimum cutting temperature medium and the aortic root was sectioned at a thickness of 8 µm. Sections were fixed in acetone, blocked with 5% goat serum in PBS for 1h30 min and incubated with anti-CD68 antibodies as described above to stain plaque macrophages. For IL-1β immunostaining sections were also incubated overnight at 4°C with a rabbit polyclonal anti-IL-1β antibody (Genetex) at a concentration of 1 µg/ml. For active caspase 1 staining, CD68-stained sections were incubated for 2 hours at room temperature with fluorescent peptide-based probes for active caspase-1 (FAM-YVAD-fmk; FLICA Caspase 1 Kit 98; ImmunoChemistry Technologies) following manufacturer's

instructions. Nuclei were stained with DAPI and slides were mounted in SlowFade Gold Antifade Reagent (Life Technologies). Image acquisition was done on a Leica SP5 confocal microscope fitted with a 40× oil-immersion objective, and image analysis and fluorescent signal quantification was done using MetaMorph Microscopy Automation & Image Analysis Software (Molecular Devices). Fluorescent signal was quantified as relative integrated fluorescence intensity normalized to total plaque or CD68+ macrophage area.

In vivo inhibition of the NLRP3 inflammasome

MCC950, a small molecule inhibitor of the NLRP3 inflammasome, was synthesized as previously described (22) diluted in PBS and delivered *in vivo* at a dose of 5 mg/Kg/day via subcutaneous mini-osmotic pumps (Alzet 2004), starting four weeks after BMT. Pumps were replaced 5 weeks later to allow a continuous infusion for the entire duration of the study. Control mice were infused with PBS.

In vivo myeloid cell homing analysis

To examine myeloid cell homing into the aorta, HFHC diet-fed Mye-Tet2-KO mice and WT controls were injected twice for two days (iv) with five million nucleated BM cells obtained from MaFIA transgenic mice (Jackson Laboratories), which express GFP under the control of the myeloid-specific mouse colony stimulating factor 1 receptor (Csf1r) promoter. After 48 h, mice were euthanized, the aortic tissue was extensively perfused in situ with PBS, harvested and snap-frozen. Infiltration of GFP-expressing cells into the atherosclerotic aortic arch was evaluated by qRT-PCR analysis of GFP transcript levels in the aorta. The following primers were used: FW: CCAGGAGCGCACCATCTTCTT; RV: GTAGTGGTTGTCGGGCAGCAG (30).

SDS-PAGE and Western Blot.

Protein extracts from cultured macrophages were obtained using ice-cold lysis buffer (Cell Signaling Technologies) supplemented with protease and phosphatase inhibitors (Roche Applied Science). Equal amounts of protein lysates were resolved by SDS-PAGE. The following antibodies were used for immunoblotting: rabbit polyclonal anti-IL-1β (GeneTex), mouse monoclonal anti-NLRP3 (Clone Cryo-2, AdipoGen Life Sciences) and rabbit monoclonal anti-β-actin (Cell Signaling Technologies). An ImageQuant LAS 4000 biomolecular imaging system (GE Healthcare) was used for image acquisition and band densitometric analysis.

Analysis of histone acetylation

Histone H3 acetylation was evaluated by chromatin immunoprecipitation combined with qPCR (ChIP-qPCR) using the SimpleChIP Plus Enzymatic Chromatin Immunoprecipitation Kit (Cell Signaling Technologies) and anti-acetyl-Histone H3 antibody (EMD Millipore, Cat. No. 06-599). qPCR was performed on a CFX96 thermal cycler (Bio-Rad) using SsoAdvanced Universal SYBR Green Master Mix (Bio-Rad). ChIP-qPCR data was analyzed using the percent input method. Acetylated H3 ChIP percent input was normalized to histone H3 ChIP percent input and presented as the ratio H3Ac:H3. The following primers were used:

Gene Promoter	Position relative to TSS*	Forward Primer	Reverse Primer
IL-1β	-181	AAGTGTGTCATCGTGGTGGAA	GTGCATCTACGTGCCTACCTT
IL-6 (Ref.20)	-166	CCTGCGTTTAAATAACATCAG CTTTAGCTT	GCACAATGTGACGTCGTTTAGCAT CGAA

* With respect to the 5' end of the downstream primers. Based on GRCm38.p3 C57BL/6J

Analysis of DNA hydroxymethylation

Global 5-hmC levels in genomic DNA isolated from blood cells or peritoneal macrophages were evaluated by ELISA, following manufacturer's instructions (Epigentek, MethylFlash Global DNA Hydroxymethylation ELISA Easy Kit).

Statistical analysis

Data are shown as mean ± SEM unless otherwise stated. Statistical significance of differences in experiments with two groups and only one variable was assessed by unpaired Student's *t* tests (with Welch correction for unequal variance when appropriate) or Mann-Whitney U Tests. Differences in experiments with more than one independent variable were evaluated by two-way analysis of variance (ANOVA) with post-hoc Sidak's or Tukey's multiple comparison tests. Results of ITT experiments were evaluated by two-way repeated measures ANOVA. All statistical tests were performed using GraphPad Prism software (GraphPad Software Inc.).

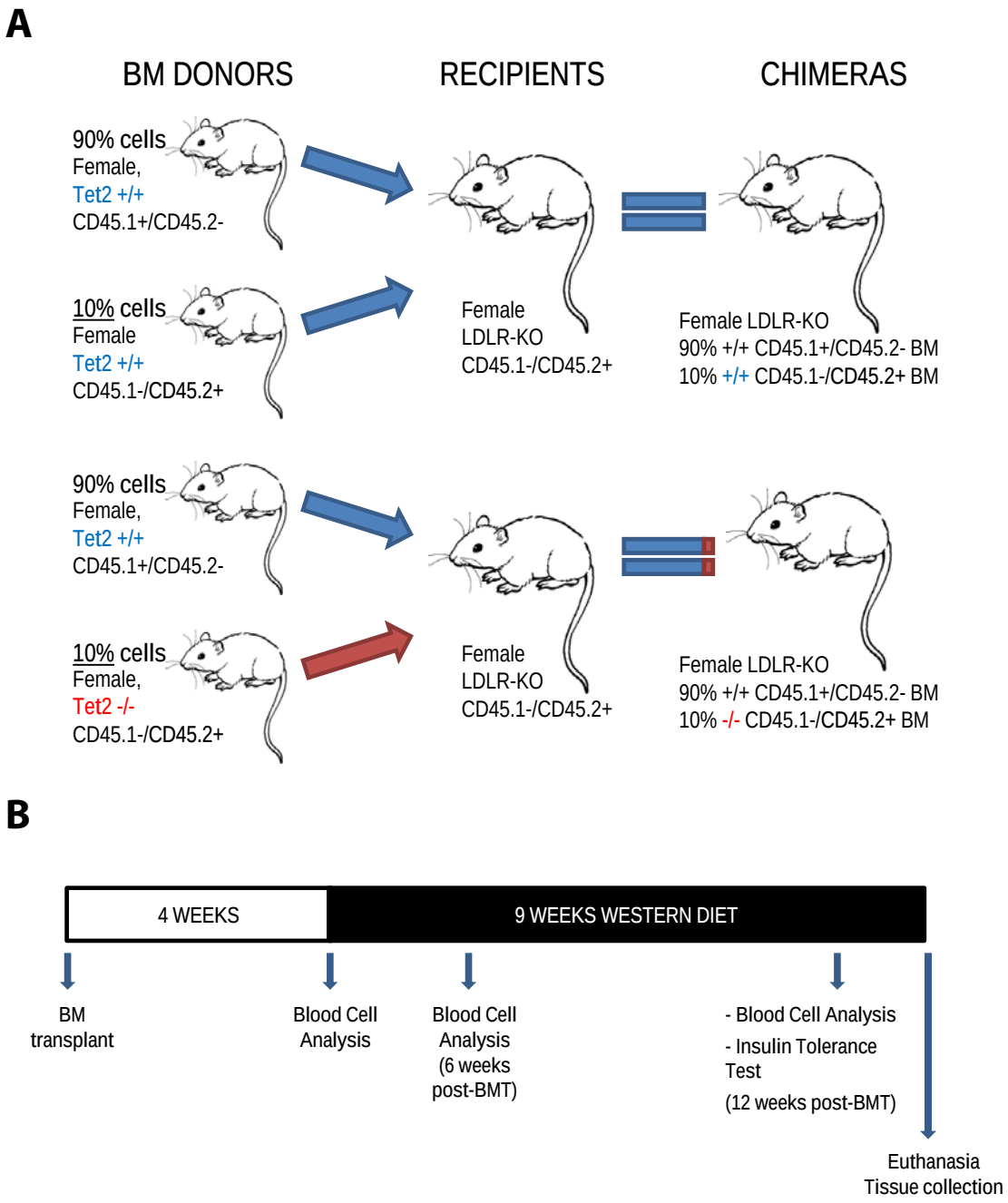

Fig. S1

Research strategy to study the role of clonal hematopoiesis associated with Tet2 deficiency in atherosclerosis development in hyperlipidemic mice. A. Competitive bone marrow transplantation strategy. **B.** Timeline of bone marrow transplantation and hematological, metabolic and atherosclerosis studies.

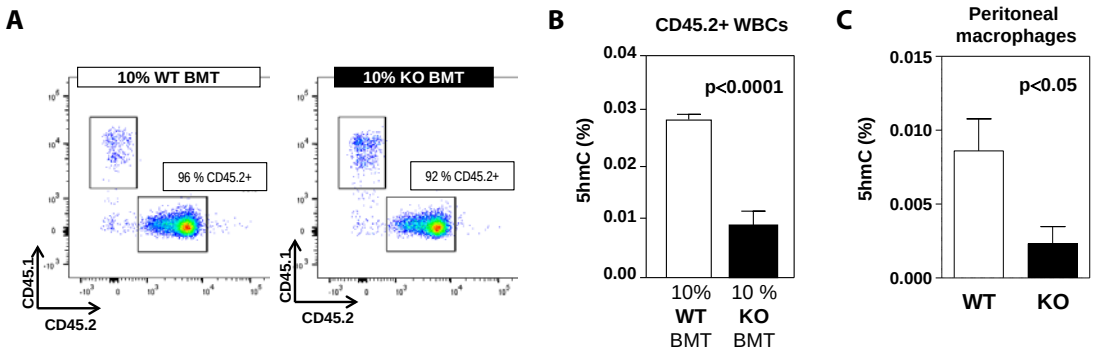

Fig. S2

Reduced 5-hydroxymethylation in Tet2-deficient cells. A. Representative images of the flow cytometry analysis of the purity of the magnetically-sorted CD45.2+ WBC fractions from 10% KO-BMT mice and WT controls analyzed in Fig.1C. **B.** Percentage of 5hmC in genomic DNA isolated from CD45.2+ WBCs of HFHC-fed 10% WT-BMT (n=4) and 10% KO-BMT mice (n=6), quantified by ELISA. **C.** Percentage of 5hmC in genomic DNA isolated from thioglycollate-elicited peritoneal macrophages obtained from Tet2-/- mice (n=4) and +/+ controls (n=5), quantified by ELISA.

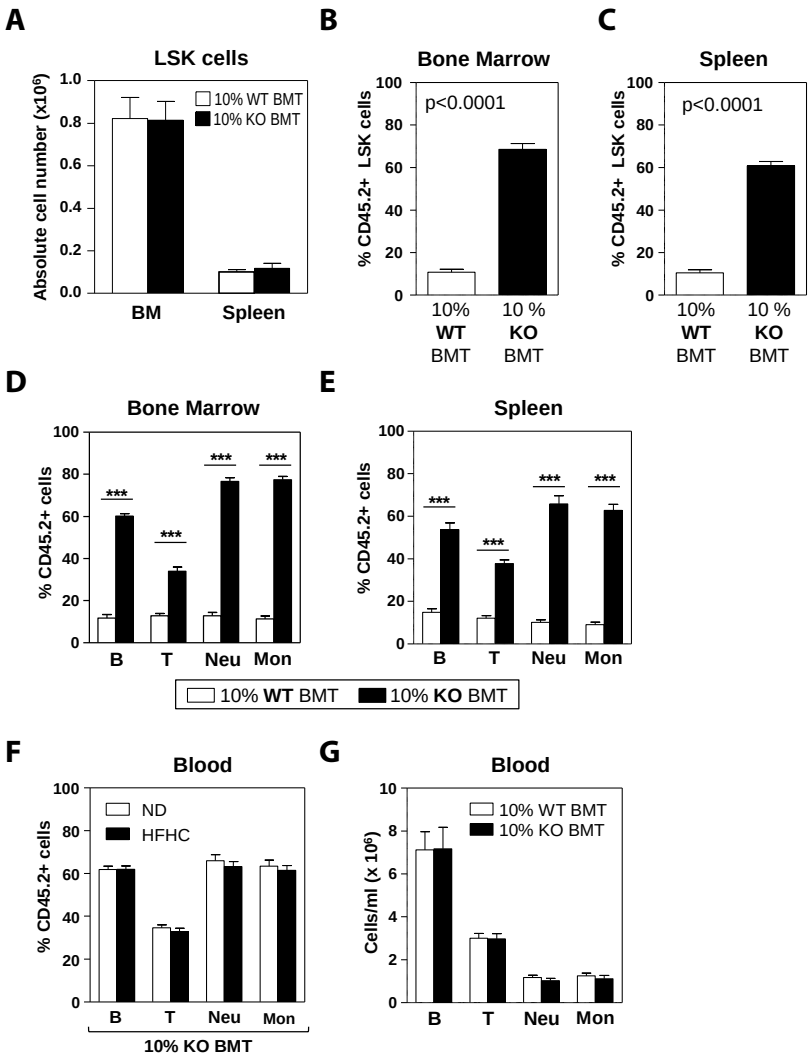

Fig. S3

Expansion of CD45.2+ HSPCs after competitive bone marrow transplantation. A. Absolute numbers of Lin-, Sca1+, Kit+ (LSK) cells in bone marrow and spleen of 10% KO-BMT mice and WT controls (n=7 per genotype) 13 weeks post-BMT (9 weeks on HFHC diet), quantified by flow cytometry. **B, C.** Percentage of CD45.2+ LSK cells in bone marrow (B) and spleen (C) of 10% KO-BMT mice (n=14) and WT controls (n=11) 13 weeks post-BMT (9 weeks on HFHC diet), quantified by flow cytometry. **D, E**. Percentage of CD45.2+ cells within the main hematopoietic lineages in bone marrow (D) and spleen (E) of 10% KO-BMT mice (n=14) and WT controls (n=11) 13 weeks post-BMT (9 weeks on HFHC diet), quantified by flow cytometry. **F**. Percentage of CD45.2+ cells within the main hematopoietic lineages in peripheral blood of 10% KO-BMT 13 weeks post-BMT (9 weeks on ND or HFHC diet, n=8-18 per condition), quantified by flow cytometry. **G.** Absolute cell numbers of main WBC populations in peripheral blood of 10% KO-BMT mice (n=14) and WT controls (n=11) 13 weeks post-BMT (9 weeks on HFHC diet), quantified by flow cytometry. Statistical significance was evaluated by two-tailed unpaired Student t tests (B, C) and 2-way ANOVA with Sidak multiple comparison tests (D-G, ***p<0.001).

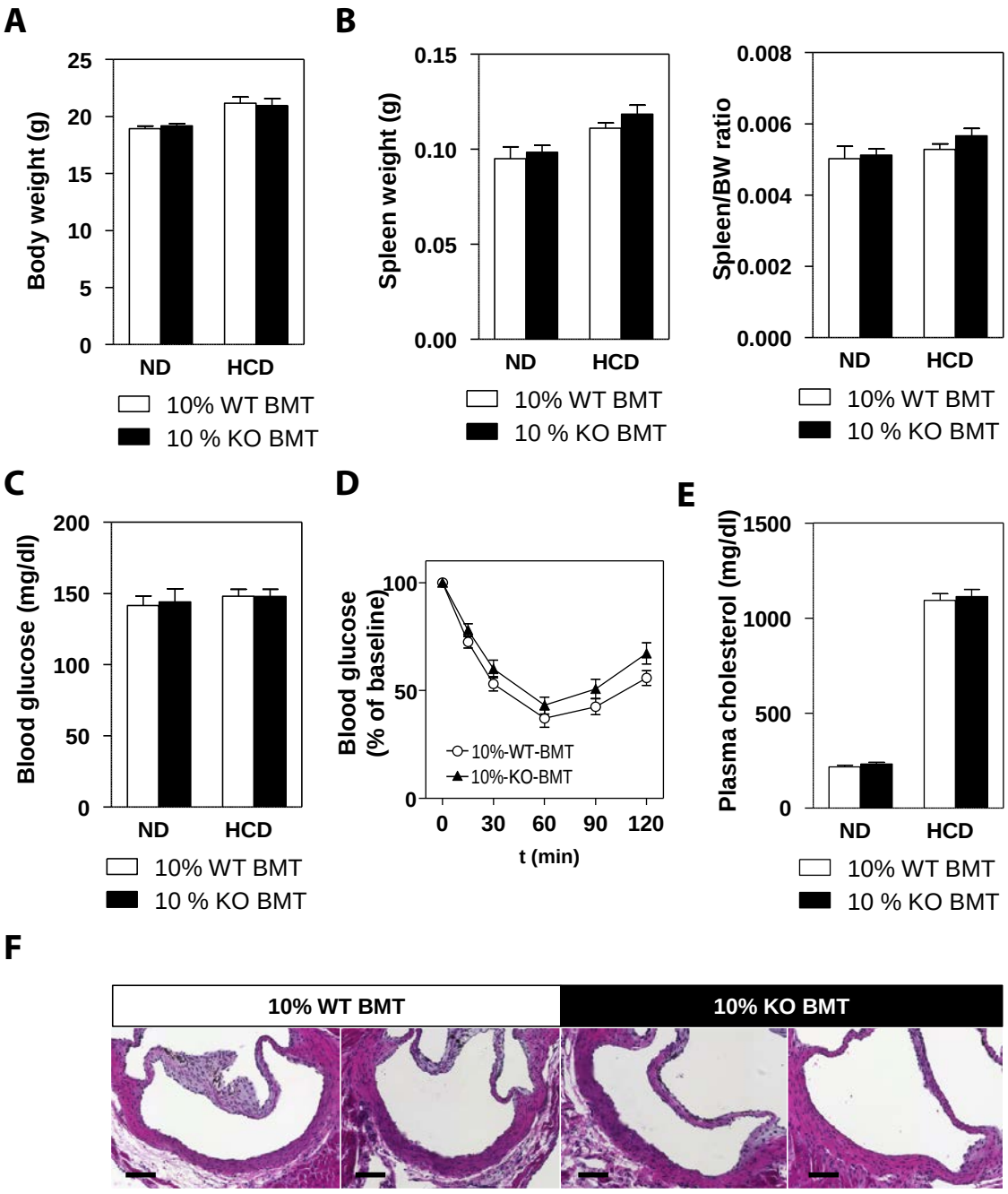

Fig. S4

A-C. Body weight (A), spleen weight and spleen/body weight ratio (B), and blood glucose levels (C) in *ad libitum*-fed 10% KO-BMT mice and WT controls after 9 weeks on ND or HFHC diet (n=8-17 per group). **D**. Insulin tolerance test in 10% KO-BMT mice (n=8) and WT controls (n=11) after 8 weeks on HFHC diet. **E**. Plasma cholesterol levels in *ad libitum*-fed 10% KO-BMT mice and WT controls after 9 weeks on ND or HFHC diet. **F**. Representative images of hematoxylin/eosin-stained aortic root sections from 10% KO-BMT mice and WT controls fed ND (scale bar: 100 µm). Statistical significance was evaluated by 2-way ANOVA with Sidak multiple comparison tests (A, B, C and E) and by repeated measures 2-way ANOVA (D).

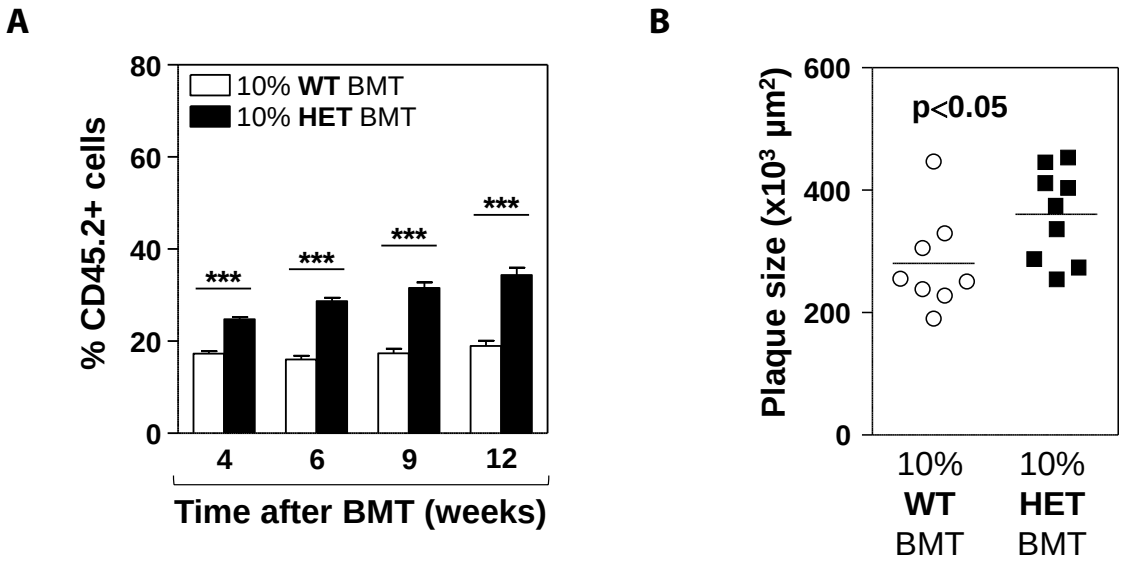

Fig. S5

Clonal expansion of Tet2-heterozygous hematopoietic cells is sufficient to accelerate atherosclerosis. Ldlr-/- mice were transplanted with bone marrow cell suspensions containing 10 % CD45.2+ Tet2+/- cells (10% HET-BMT, n=9) or 10% CD45.2+ Tet2+/+ cells (10% WT-BMT, n=9) and 90 % CD45.1+ Tet2+/+ cells. **A**. Percentage of CD45.2+ white blood cells (WBC) in peripheral blood, evaluated by flow cytometry. **B**. Aortic root plaque size, average of five independent sections.

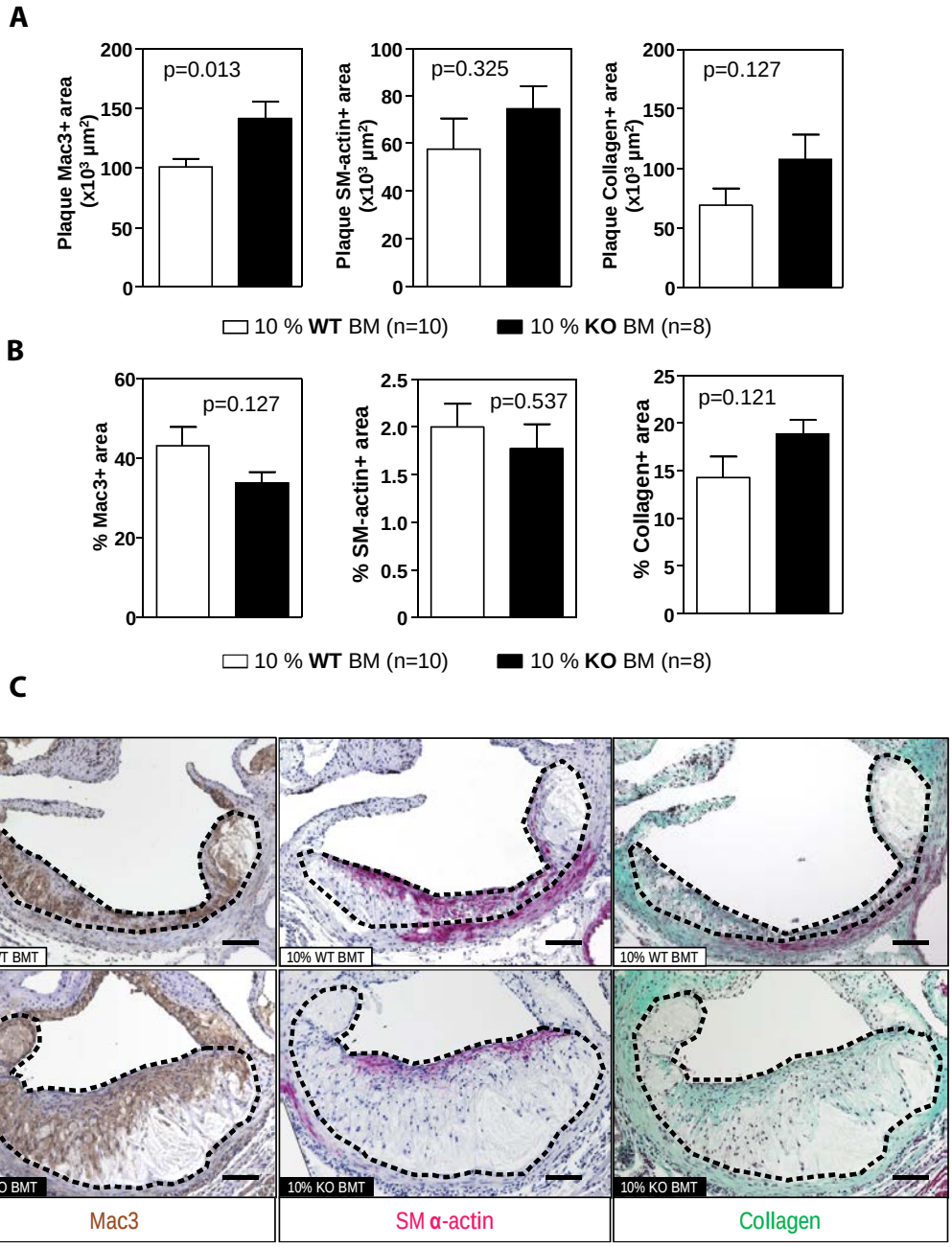

Fig. S6

Effects of clonal expansion of Tet2-deficient cells on atherosclerotic plaque composition. 10% KO BMT mice (n=8) and WT controls (n=10) were fed HFHC diet for 9 weeks. Immunohistochemical staining was used to evaluate plaque content of macrophages (Mac3+ area) and vascular smooth muscle cells (SM-α-actin+ area). A modified Masson Trichome staining was used to quantify collagen content in the plaque. **A.** Plaque composition quantified as absolute intimal content of each component. **B.** Plaque composition quantified as percentage of total lesion area of each component. **C.** Representative images of plaques in 10 % KO-BMT mice are shown for each staining and atherosclerotic plaques are delineated by discontinuous lines (scale bar: 100 µm). Statistical significance was evaluated by two-tailed unpaired Student t tests.

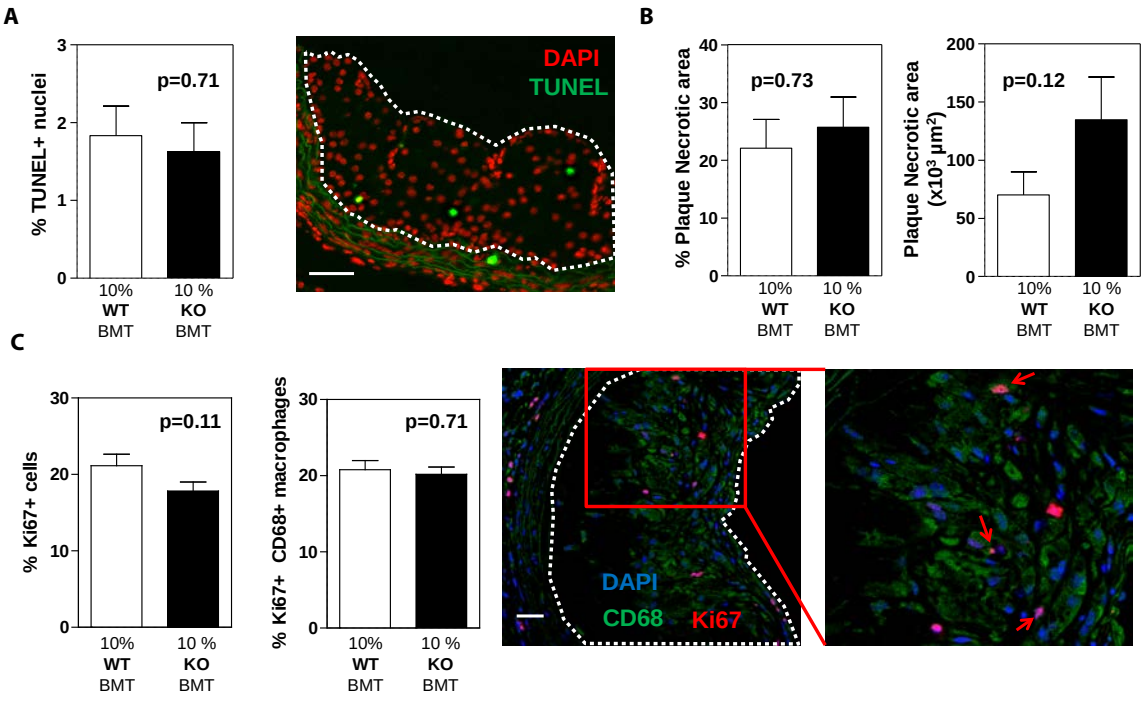

Fig. S7

Clonal expansion of Tet2 deficient cells does not affect plaque cell death or macrophage proliferation. 10% KO BMT mice and WT controls were fed HFHC diet for 9 weeks. **A.** TUNEL staining to detect apoptotic cells (n=10 10% WT-BMT mice, n=8 10% KO-BMT mice). An image representative of plaque cell apoptosis in 10% KO-BMT mice is shown; atherosclerotic plaque is delineated by discontinuous lines (scale bar: 50 µm). **B.** Necrotic core extension, quantified as collagen-free acellular area in Masson Trichrome-stained sections (n=10 10% WT-BMT mice, n=8 10% KO-BMT mice). **C.** Plaque cell proliferation, examined by immunofluorescent analysis of the proliferating cell-specific antigen Ki67 and the macrophage marker CD68 (n=6 per genotype). An image representative of plaque cell proliferation in 10% KO-BMT mice is shown; atherosclerotic plaque is delineated by discontinuous lines (scale bar: 30 µm). Examples of proliferating (Ki67+) macrophages (Mac3+) are indicated by arrows. Statistical significance was evaluated by two-tailed unpaired Student t tests.

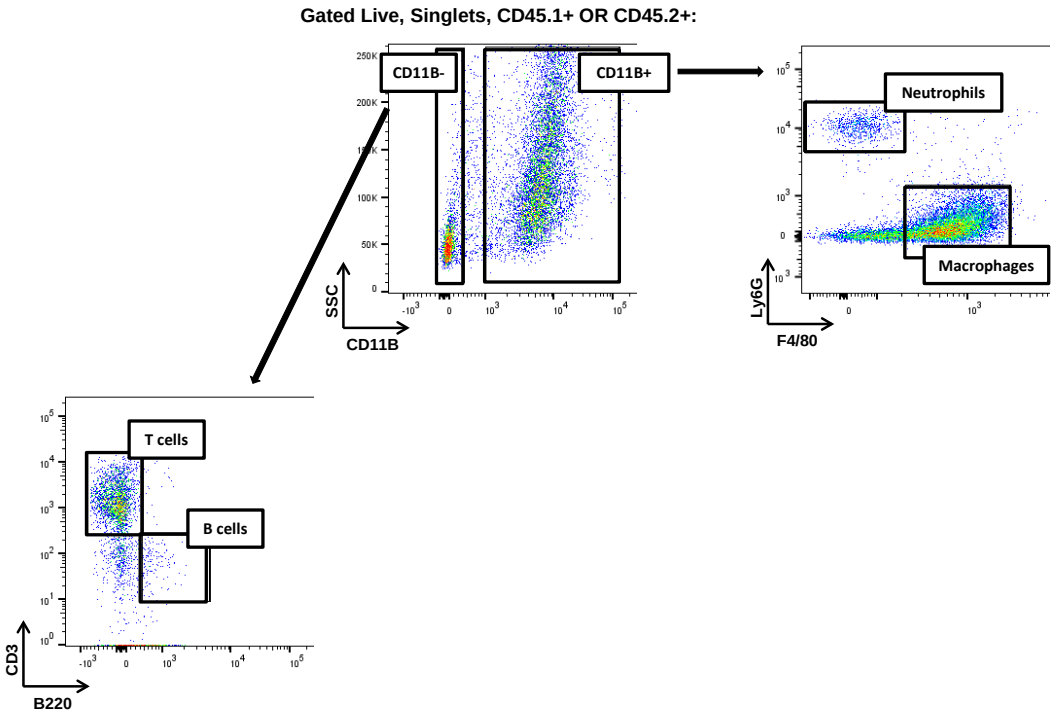

Fig. S8

Gating strategy for the flow cytometry analysis of immune cell populations in aortic arch samples (related to Fig.1F,G; the low number of neutrophils or B cells in the aortic arch at this early stage of atherosclerosis precluded the accurate analysis of CD45.2+ cells in these cell types).

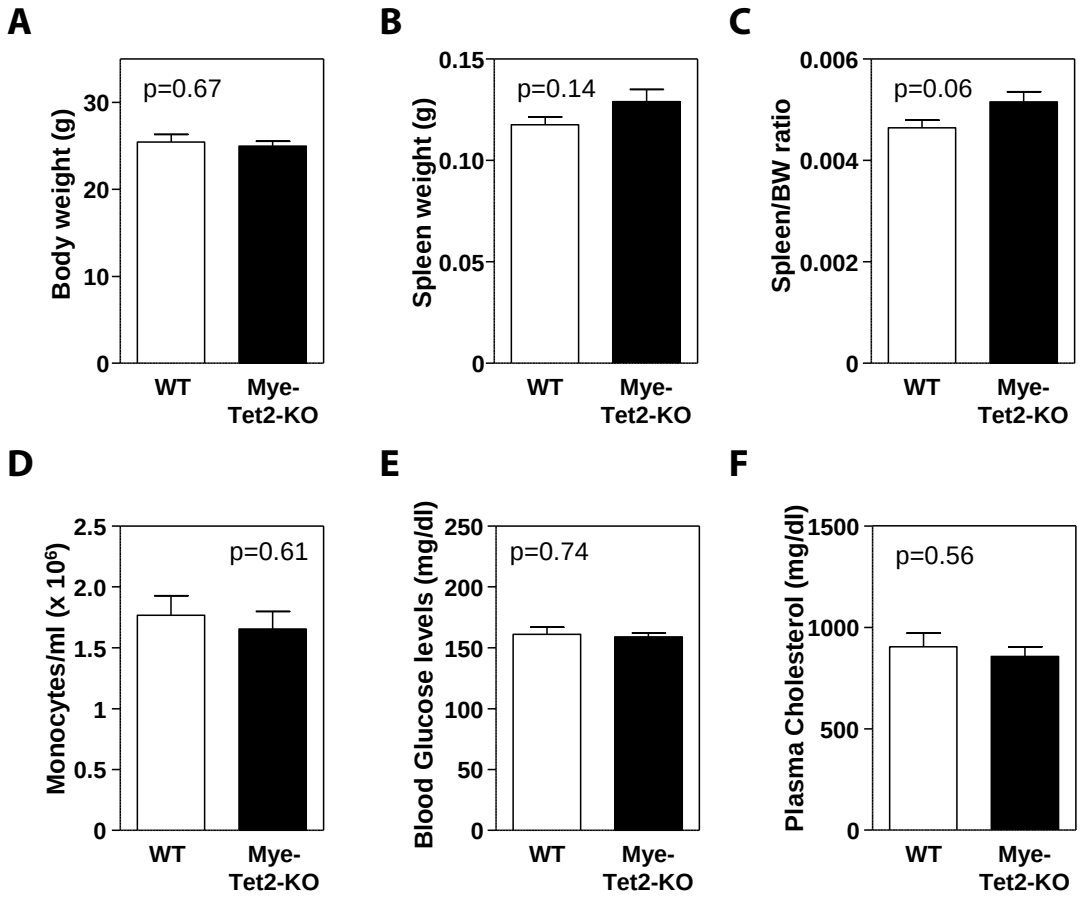

Fig. S9

Mye-Tet2-KO mice (n=10) and WT controls (n=9) were generated as described in the main text and the Materials and Methods section, and fed HFHC diet for 10 weeks. **A.** Body weight. **B.** Spleen weight. **C**. Spleen/body weight ratio. **D.** Blood monocytes, quantified by flow cytometry. **E**. Blood glucose levels in *ad libitum* fed mice. **F.** Plasma cholesterol levels in in *ad libitum* fed mice. Statistical significance was evaluated by two-tailed unpaired Student t tests.

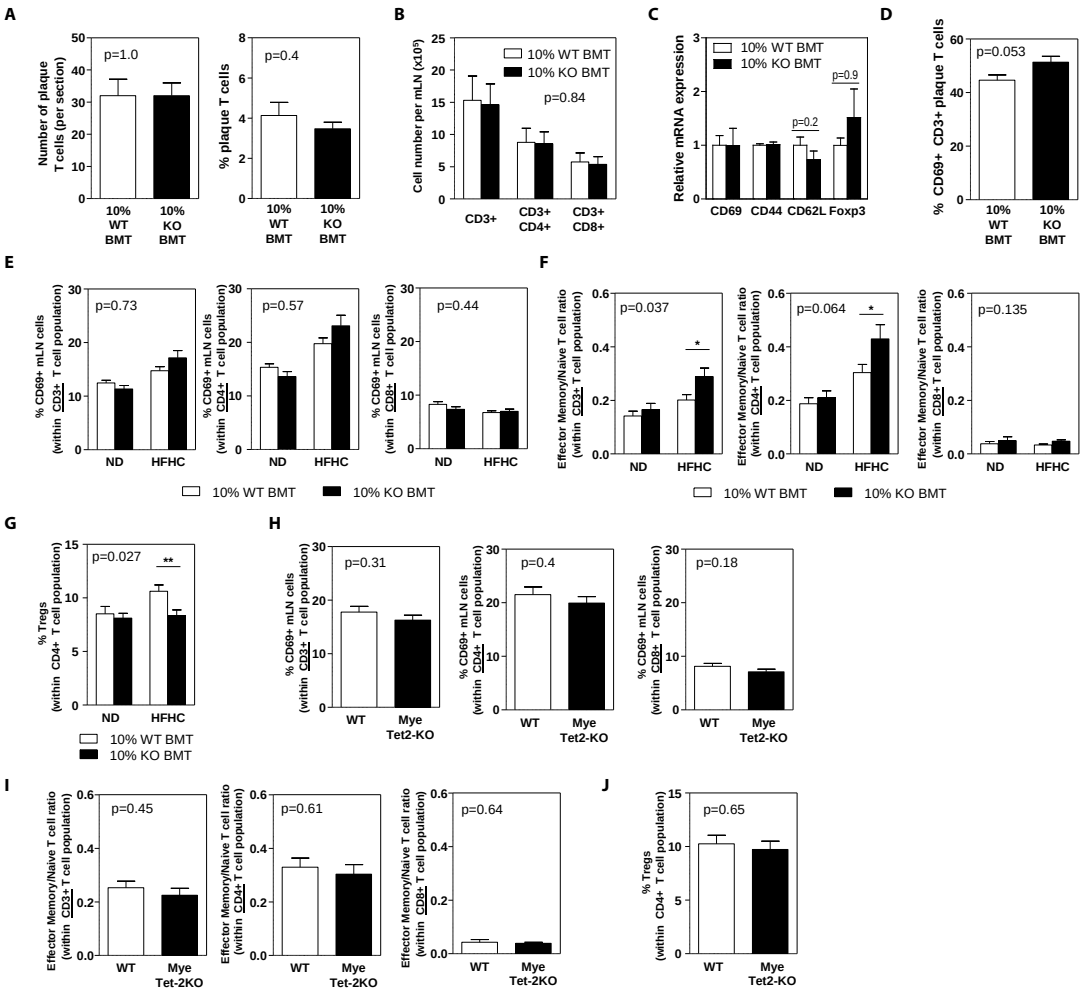

Fig. S10

Effects of hematopoietic Tet2 deficiency on T cell subsets in aorta and aorta-draining mediastinal lymph nodes. A-G. 10% KO-BMT mice and WT controls were fed ND or HFHC diet for 9 weeks (n=8-10 per genotype and condition). **A.** CD3+ T cell content in atherosclerotic plaques, analyzed by immunofluorescent staining and fluorescence microscopy of histological sections of aortic root. **B.** T cell numbers in aorta-draining mediastinal lymph nodes (mLNs), evaluated by flow cytometry. **C.** qRT-PCR analysis of various T cell activation markers in aortic arch samples. **D.** Percentage of activated (CD69+) T cells in atherosclerotic aortic arches, evaluated by flow cytometry. **E.** Percentage of activated (CD69+) T cells in mLNs, evaluated by flow cytometry. **F.** Effector memory/naïve T cell ratios in mLNs, evaluated by flow cytometry. Effector memory T cells were identified as $CD44^{Hi}$ $CD62L^{-}$ and naïve T cells as $CD44^{Lo}$ $CD62L^{+}$. **G.** Percentage of regulatory T cells (Tregs) in mLNs, evaluated by flow cytometry. Tregs were identified as $CD4^{+}$ $CD127^{Lo}$ $CD25^{+}$ $FoxP3^{+}$. **H-J**. Mye-Tet2-KO mice (n=10) and WT controls (n=8) were fed HFHC diet for 10 weeks. Percentages of activated (CD69+) T cells (**H**), effector memory/naïve T cell ratios (**I**) and Tregs (**J**) in mLNs are shown. Statistical significance was evaluated by two-tailed unpaired Student t tests or Mann Whitney tests in A, C, D and H-J; and by 2-way ANOVA (p value for genotype effect is shown) with Sidak multiple comparison tests (*p<0.05, **p<0.01) in B, E, F and G.

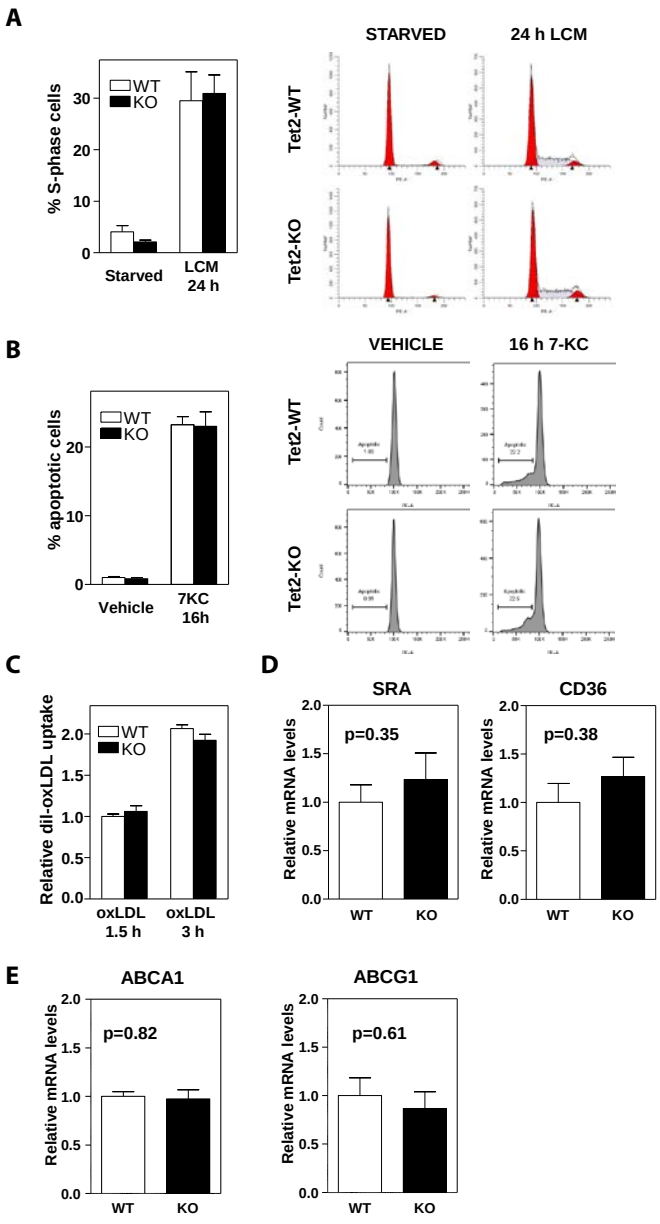

Fig. S11

Effects of Tet2 deficiency on cultured macrophage proliferation, apoptosis and oxLDL uptake. Bone-marrow-derived (A) or peritoneal (B-E) macrophages were obtained from Tet2-/- mice or +/+ controls (n=3 mice/genotype). **A**. Cell-cycle progression analysis by propidium iodide staining and flow cytometry after synchronization of macrophages in G0-phase by 36 h of MCSF deprivation and subsequent re-stimulation.with 15 % L929-cell conditioned medium (LCM) as a source of MCSF. **B**. Quantification of apoptotic macrophages after 16 hours of treatment with 20 µg/ml 7-ketocholesterol, identified by flow cytometry as the sub-G0/G1 population after propidium iodide staining. **C**. Quantification of fluorescent DiI-oxLDL uptake by macrophages, detected by flow cytometry. **D, E**. qRT-PCR analysis of expression of the scavenger receptors SR-A and CD36 (**D**) and the cholesterol efflux transporters ABCA1 and ABCG1 (**E**). Statistical significance was evaluated by 2-way ANOVA with Sidak multiple comparison tests (A-C) and two-tailed unpaired Student t tests (D-E).

A.

Number of differentially expressed genes	Untreated		LPS/IFNγ-treated (10h)	
	# up-regulated	# down-regulated	# up-regulated	# down-regulated
Q<0.5, FC ≥1.5 or ≤-1.5	4	17	479	331
Q<0.05, FC ≥1.5 or ≤-1.5	0	0	306	169
Q<0.05, FC ≥2 or ≤-2	0	0	79	38
Q<0.01, FC ≥1.5 or ≤-1.5	0	0	45	17

B.

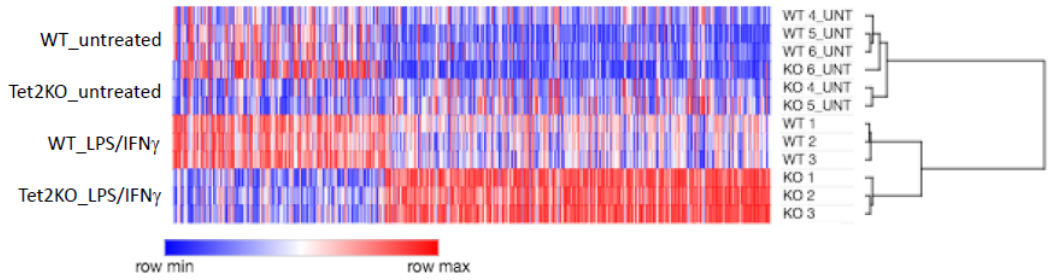

Fig. S12

Tet2-/- macrophages showed significant changes in overall gene expression compared to +/+ controls after a 10-hour treatment with a combination of 10 ng/ml LPS and 2 ng/ml IFNγ, but not at baseline. **A.** Number of differentially expressed genes between Tet2-/- macrophages and +/+ controls at baseline (untreated) and after LPS/IFNγ treatment using various statistical cutoffs. Genes with q<0.05 and fold change ≥1.5 or ≤-1.5 were considered as statistically significantly different between the conditions and were used for further analysis (highlighted in red). **B.** Heat map of genes that were significantly differently expressed in Tet2+/+ (WT) and -/- (KO) macrophages after LPS/IFNγ treatment. While distinct clustering and expression pattern were found for the samples in Tet2-WT and -KO macrophages after 10hr LPS/IFNγ treatment (WT_LPS/IFNγ vs. Tet2KO_ LPS/IFNγ), no differences were found in the Tet2-WT and Tet2-KO macrophages at baseline, untreated state (WT_untreated vs. Tet2KO_ untreated).

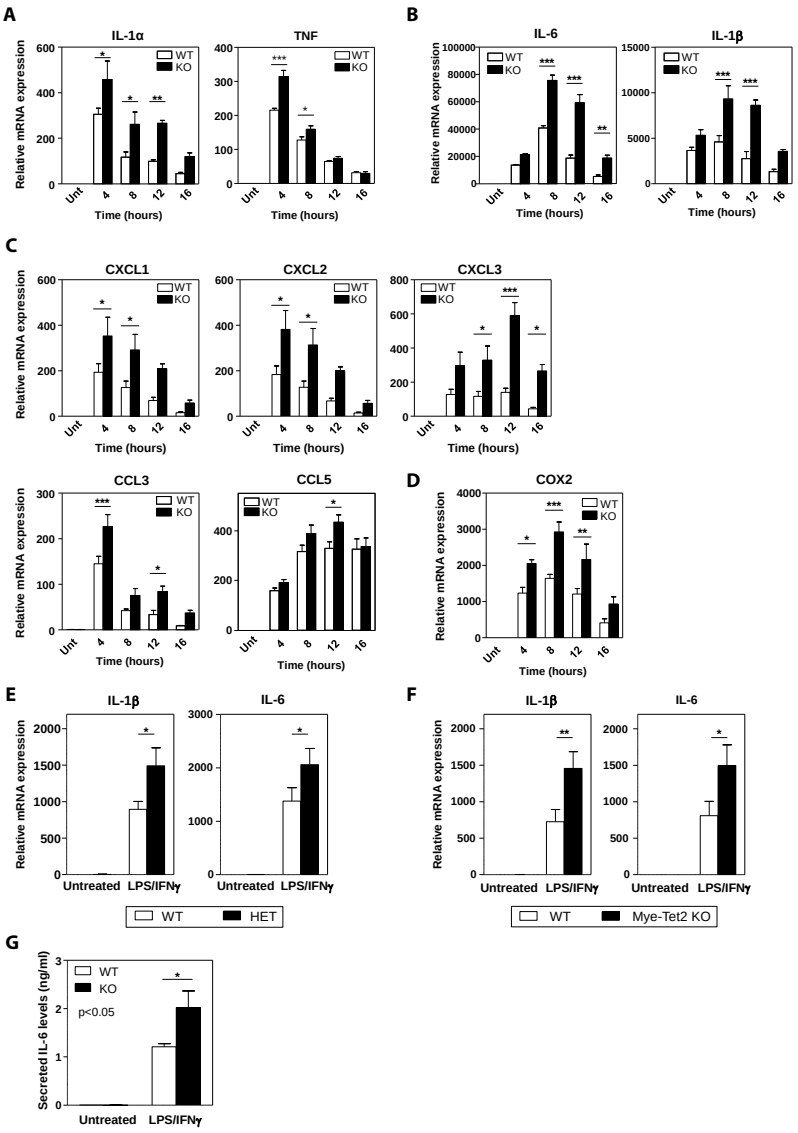

Fig. S13

Effects of Tet2 deficiency on the expression of pro-inflammatory cytokines/chemokines by cultured macrophages. A-D. Peritoneal macrophages were isolated from Tet2-/- mice or +/+ controls (n=4 mice/genotype) and treated with 10 ng/ml LPS and 2 ng/ml IFNγ (A, C, D) or 100 ng/ml LPS and 20 ng/ml IFNγ (B). Transcript levels of proinflammatory cytokines (A, B), chemokines (C) and enzymes (D) were quantified by qRT-PCR. **E.** Peritoneal macrophages were isolated from Tet2+/- mice or +/+ controls (n=6 mice/genotype) and treated with 10 ng/ml LPS and 2 ng/ml IFNγ for 8 hours. Gene expression was analyzed by qRT-PCR. **F.** Peritoneal macrophages were isolated from Mye-Tet2-KO mice (n=6) and WT controls (n=4) and treated with 10 ng/ml LPS and 2 ng/ml IFNγ for 8 hours. Gene expression was analyzed by qRT-PCR. **G.** Peritoneal macrophages were isolated from Tet2-/- mice or +/+ controls (n=3 mice/genotype) and treated with 10 ng/ml LPS and 2 ng/ml IFNγ for 16 hours. IL-6 protein levels in cell culture supernatants were evaluated by ELISA. Statistical significance was evaluated by 2-way ANOVA with Sidak multiple comparison tests (*p<0.05, **p<0.01, ***p<0.001).

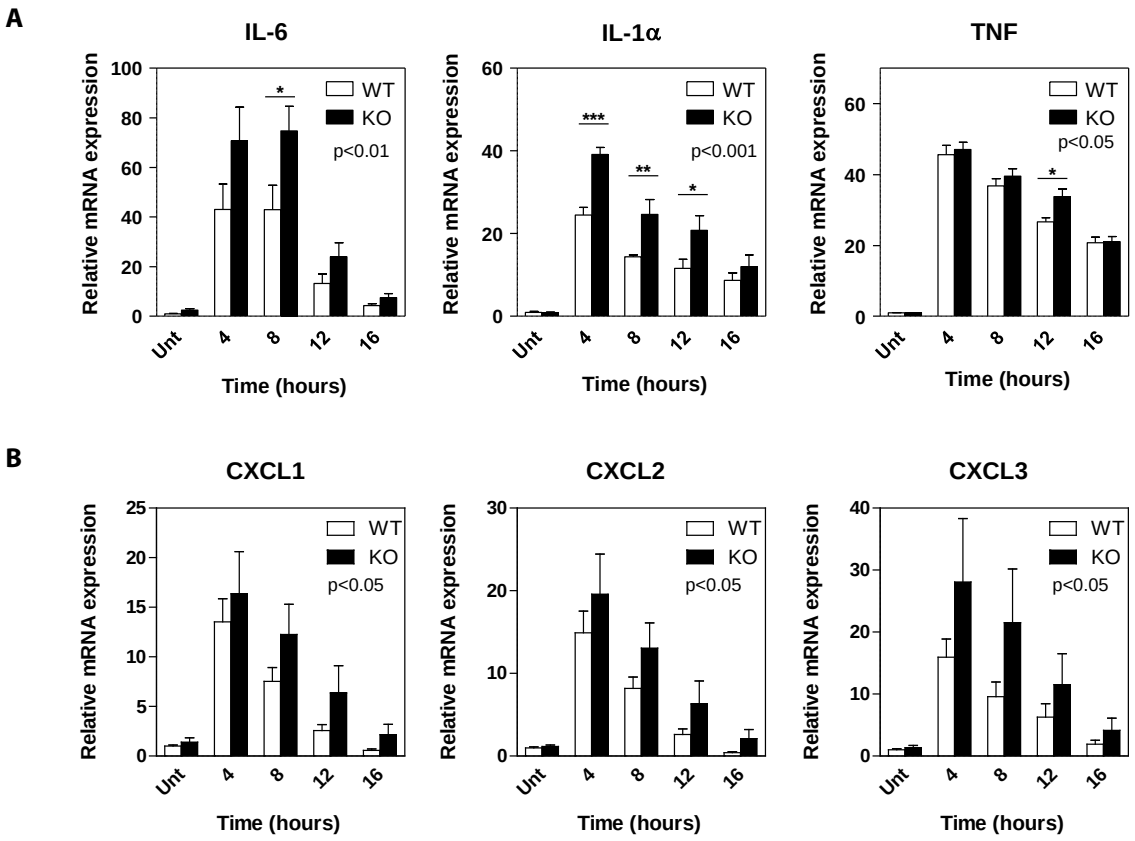

Fig. S14

Effects of Tet2 deficiency on the expression of pro-inflammatory cytokines/chemokines by cultured macrophages in the presence of low doses of oxLDL, TNF and IFNγ. Peritoneal macrophages were obtained from Tet2-KO mice or WT controls (n=6 mice/genotype) and treated with 25 µg/ml oxLDL, 5 ng/ml TNF and 2 ng/ml IFNγ. Gene expression of selected pro-inflammatory cytokines (A) or chemokines (B) was analyzed by qRT-PCR. Statistical significance was evaluated by 2-way ANOVA (p value for genotype effect is shown) with Sidak multiple comparison tests (*p<0.05, **p<0.01, ***p<0.001).

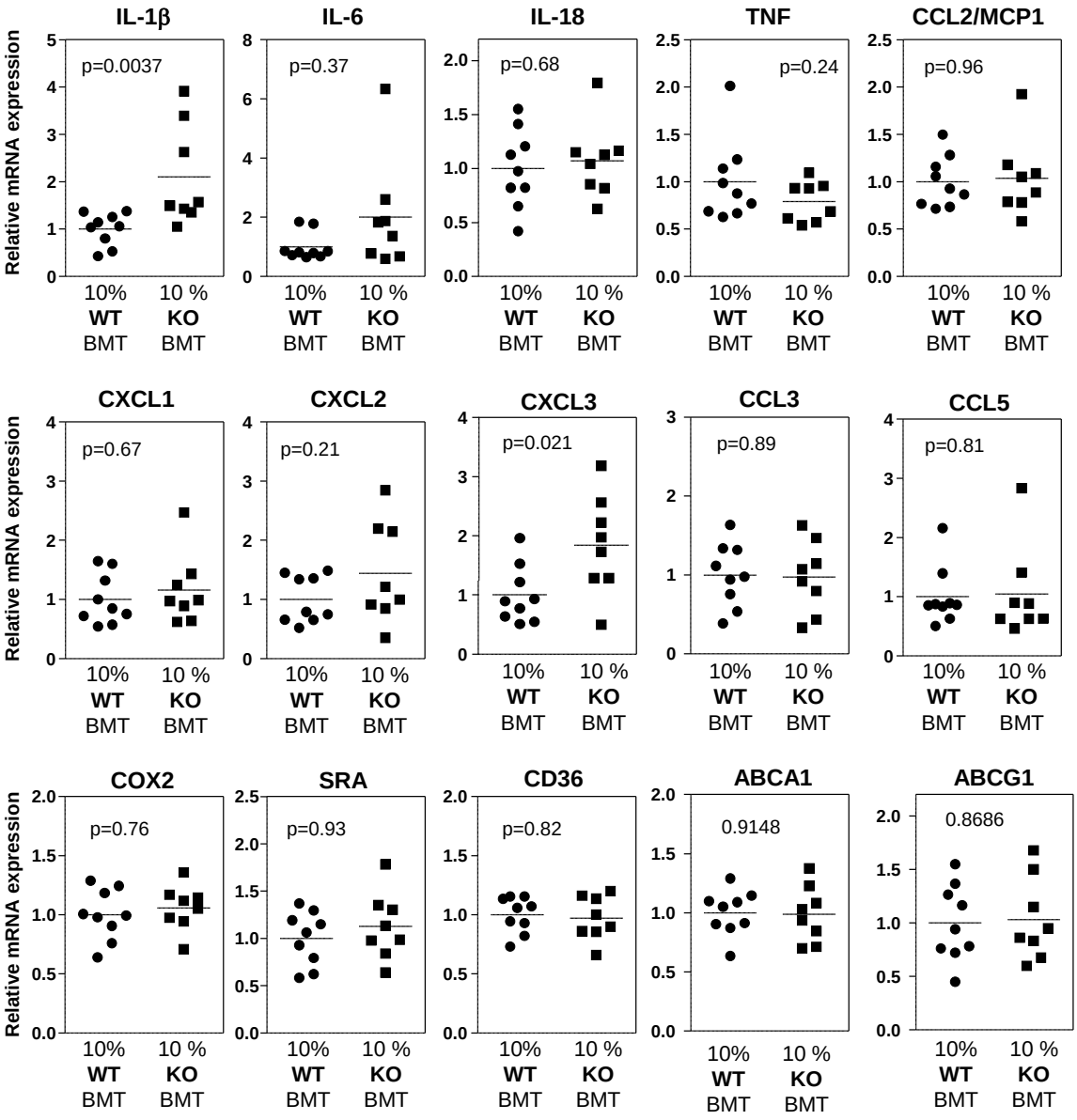

Fig. S15

Effects of Tet2-deficient hematopoietic cell expansion on the expression of pro-inflammatory cytokines, chemokines and cholesterol trafficking regulators in the atherosclerotic vascular wall. Aortic arch samples were obtained from 10% WT-BMT mice (n=9) or 10% KO-BMT mice (n=8) and gene expression was analyzed by qRT-PCR analysis. Statistical significance was evaluated by two-tailed unpaired Student t tests (with Welch's correction for IL-1β analysis) or by Mann Whitney tests for data that did not pass the D'Agostino and Pearson normality test).

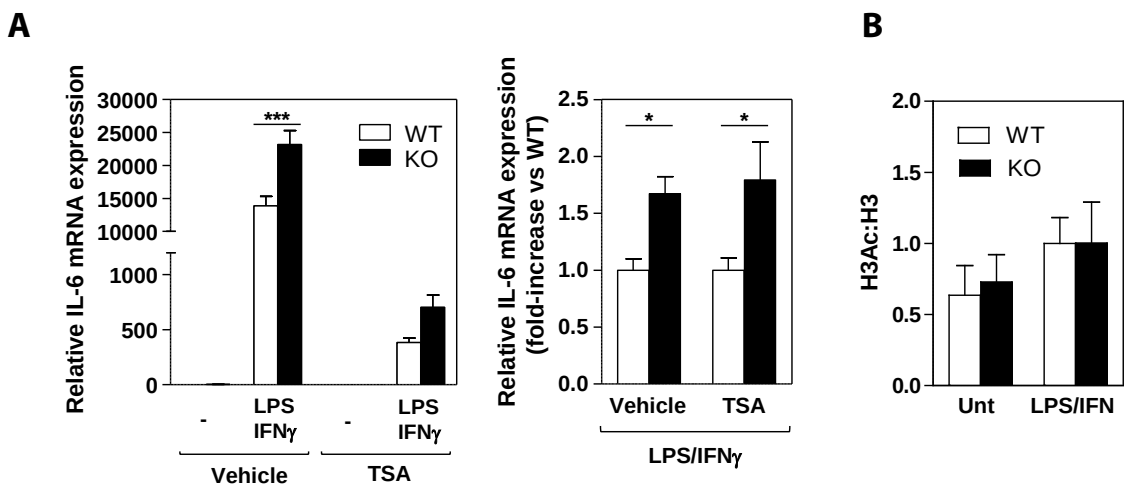

Fig. S16

A. qRT-PCR analysis of IL-6 expression in peritoneal macrophages isolated from Tet2-/- or +/+ mice (n=3 mice/genotype) and treated for 8 hours with 10 ng/mL LPS and 2 ng/ml IFNγ in the absence or presence of 0.5 μM Trichostatin A (TSA). **B.** ChIP-qRT-PCR analysis of H3 acetylation in the IL-6 promoter of macrophages isolated from Tet2-/- or +/+ mice (n=6-8 per genotype and condition) after 10 hours of LPS/IFNγ treatment. Statistical significance was evaluated by 2-way ANOVA with Sidak multiple comparison tests (*$p<0.05$, ***$p<0.001$).

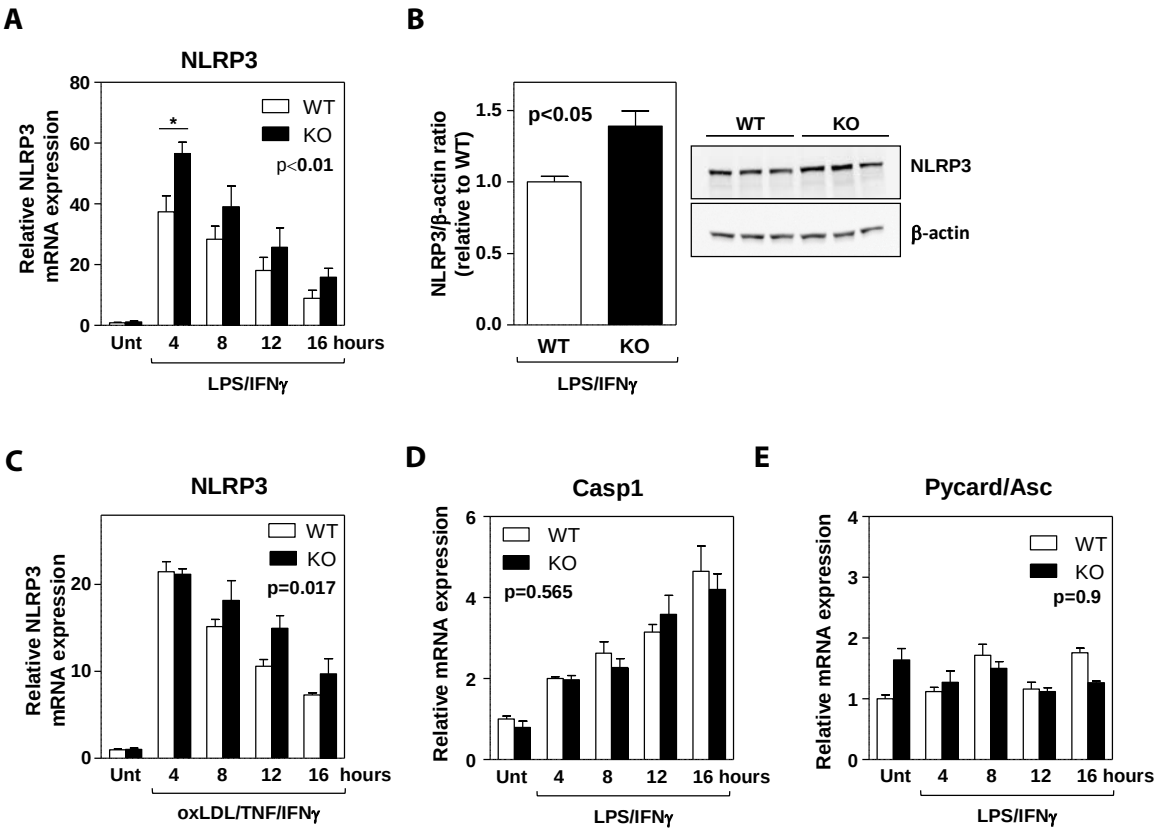

Fig. S17

A. qRT-PCR analysis of NLRP3 transcript levels in peritoneal macrophages isolated from Tet2-/- mice or +/+ controls (n=4 per genotype) and treated with 10 ng/ml LPS and 2 ng/ml IFNγ. **B.** Western Blot analysis of NLRP3 protein levels in peritoneal macrophages isolated from Tet2-/- mice and +/+ controls (n=3 per genotype) and treated for 6 hours with LPS/IFNγ. **C.** qRT-PCR analysis of NLRP3 transcript levels in peritoneal macrophages isolated from Tet2-/- mice or +/+ controls (n=4 per genotype) and treated with 25µg/ml oxLDL, 5 ng/ml TNF and 2 ng/ml IFNγ. **D, E.** qRT-PCR analysis of gene expression in LPS/IFNγ-treated macrophages isolated from Tet2-/- mice and +/+ controls (n=3 per genotype). Statistical significance was evaluated by 2-way ANOVA (p value for genotype effect is shown) with Sidak multiple comparison test in A, C, D, E (*p<0.05); and by two-tailed unpaired Student t tests in B.

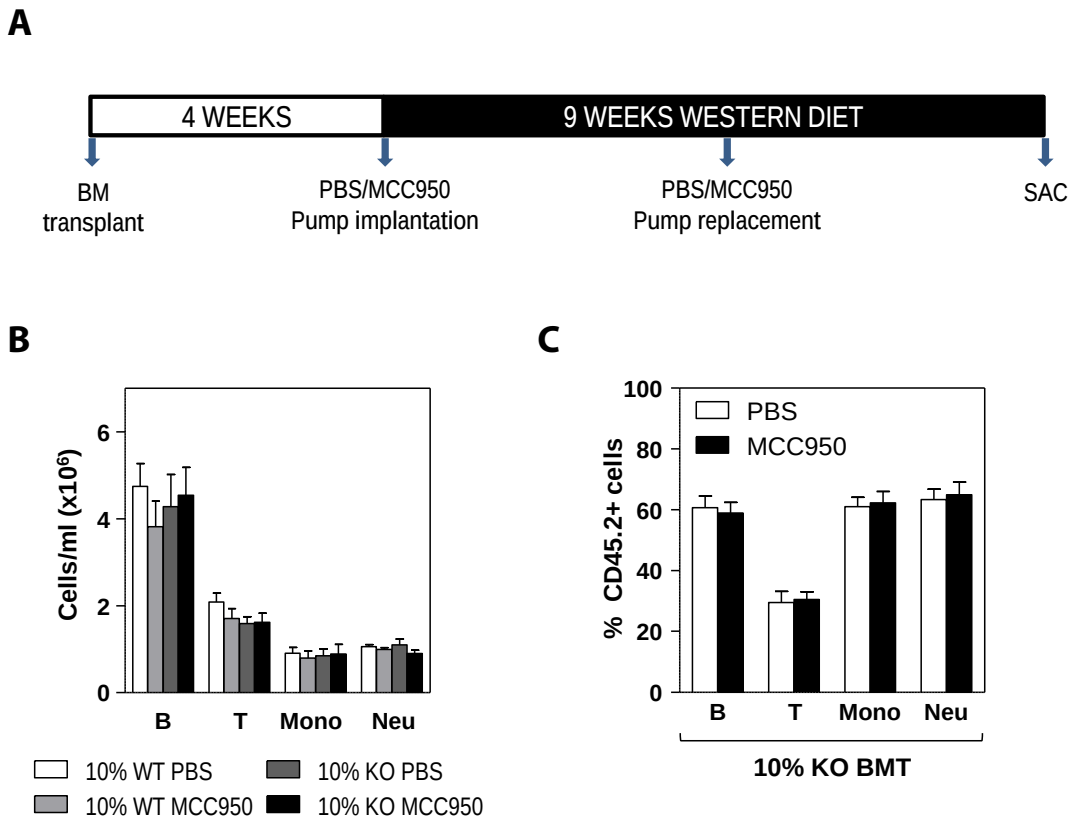

Fig. S18

A. Timeline of bone marrow transplantation, HFHC diet feeding and subcutaneous osmotic pump implantation/replacement. **B.** Absolute cell numbers of main WBC populations in peripheral blood of HFHC-fed 10% KO-BMT mice and WT controls 13 weeks post-BMT (9 weeks of PBS or MCC950 infusion), quantified by flow cytometry (n=9-11 per genotype and condition). **C.** Percentage of CD45.2+ cells within the main hematopoietic lineages in peripheral blood of 10% KO-BMT after 9 weeks of HFHC diet and infusion with PBS or MCC950, quantified by flow cytometry (n=9 per condition). Statistical significance was evaluated by 2-way ANOVA with Sidak multiple comparison tests.

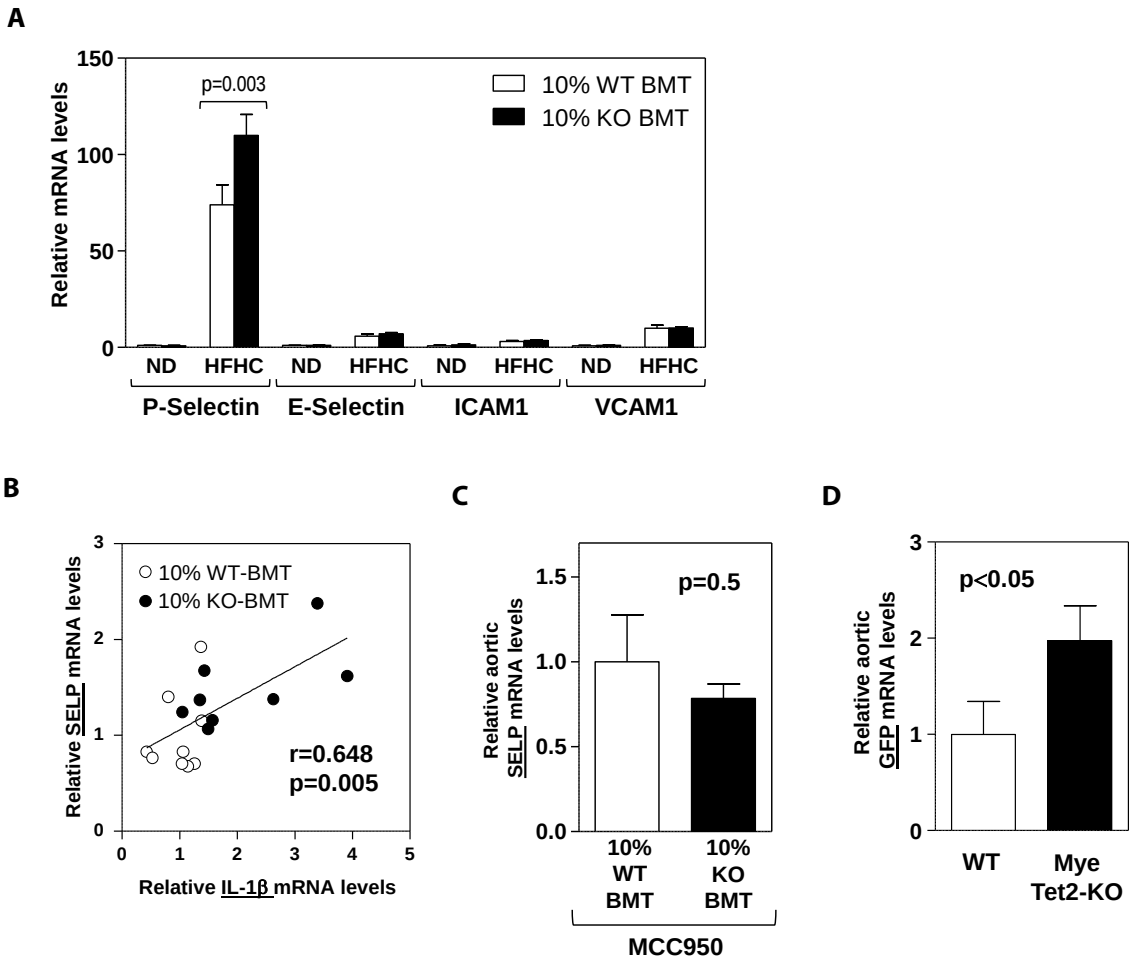

Fig. S19

Effects of hematopoietic Tet2 deficiency on endothelial adhesion molecule expression and myeloid cell recruitment to the atherosclerotic aorta. A. Aortic arch samples were obtained from 10% WT-BMT mice (n=9) or 10% KO-BMT mice (n=8) and gene expression of various endothelial adhesion molecules was analyzed by qRT-PCR. **B.** The Pearson correlation coefficient (r) was used to evaluate the association between SELP and IL-1β expression in the aortic wall of HFHC-fed 10% KO-BMT mice and WT controls. **C.** Aortic arch samples were obtained from HFHC-fed, MCC950-infused 10% WT-BMT mice (n=5) or 10% KO-BMT mice (n=6) and P-Selectin transcript levels were analyzed by q-RT-PCR. **D.** qRT-PCR analysis of GFP transcript levels was used to evaluate aortic recruitment of GFP+ (Tet2-WT) myeloid cells after adoptive transfer to HFHC-fed Mye-Tet2-KO (n=10) and WT controls (n=8). Statistical significance was evaluated by 2-way ANOVA with Sidak multiple comparison tests in A, by two-tailed unpaired Student t test with Welch's correction in C, and by Mann Whitney test in D.